

Transcript profiling of conifer pathosystem: response of *Pinus sylvestris* root tissues to pathogen (*Heterobasidion annosum*) invasion

¹Aleksandra Adomas*, ¹Gregory Heller, ¹Guosheng Li, ¹Åke Olson, ²Tzu-Ming Chu, ³Jason Osborne, ⁴Deborah Craig, ⁴Len van Zyl, ²Russ Wolfinger, ⁴Ron Sederoff, ⁵Ralph A. Dean, ¹Jan Stenlid, ¹Roger Finlay, ¹Frederick O. Asiegbu

¹Department of Forest Mycology and Pathology, Swedish University of Agricultural Sciences, Box 7026, Uppsala Sweden; ²SAS Institute, Cary NC 27513, USA; ³Department of Statistics, Box 8203, North Carolina State University, Raleigh NC 27695 USA ⁴Forest Biotechnology Laboratory, Box 7247, North Carolina State University, Raleigh NC 27695, USA ⁵Fungal Genomics Laboratory, Box 7251, North Carolina State University, Raleigh NC 27695, USA

* Author for correspondence: Tel.: +46 18 67 27 98, Fax: +46 18 67 35 99, E-mail: Aleksandra.Adomas@mykopat.slu.se

Summary

The mechanisms underlying defence reactions to a pathogen attack though well studied in crop plants are poorly understood in conifers. To analyse changes in gene transcript levels in *Pinus sylvestris* L. root tissues infected by *Heterobasidion annosum* (Fr.) Bref. sensu stricto, a cDNA microarray containing 2109 ESTs from *P. taeda* L. was used. Mixed model statistical analysis identified 179 ESTs differentially expressed at 1, 5 or 15 days post inoculation (d.p.i.). In general, the total number of genes differentially expressed during the infection increased over time. The most abundant group of genes up-regulated upon infection coded for enzymes involved in metabolism (phenylpropanoid pathway) and defence-related proteins with antimicrobial properties. A class III peroxidase responsible for lignin biosynthesis and cell wall thickening had increased transcript level at all time points. Real-time RT PCR verified the microarray results with high reproducibility. The similarity in expression profiling pattern observed in this pathosystem to those documented in crop pathology suggests that both angiosperms and gymnosperms might use similar genetic programs for responding to invasive growth by microbial pathogens.

Key words: antimicrobial peptide, microarray, peroxidase, phenylpropanoid pathway, pine, plant defence.

Introduction

Most conifers can be infected by the basidiomycete *Heterobasidion annosum* (Fr.) Bref. sensu lato, causative agent of a root and butt rot disease. The fungus is widely regarded as the most economically important forest pathogen in temperate regions of the northern hemisphere (Asiegbu, Adomas & Stenlid, 2005; Woodward *et al.*, 1998). Its biology including ecology and disease spread has

been intensively studied but the genetics and molecular aspects of the host response to the pathogen infection have been relatively little examined.

Typically, plant defence mechanisms comprise preformed and inducible physical and chemical barriers. Preformed physical barriers include thorns, bark and cuticular waxes and chemical defences comprise a range of antimicrobial compounds. There is a tendency for these compounds to be either concentrated in the outer cell layers of plant organs or sequestered in vacuoles or organelles in healthy plants (Osbourn, 1996). Following the recognition of a pathogen, numerous signal cascades are activated and a battery of inducible defence mechanisms is launched. Functional identification of many of the pathogen-induced genes and proteins has revealed their involvement in various biochemical pathways from both primary and secondary metabolism (Somssich & Hahlbrock, 1998). Primary metabolism supplies large carbon fluxes into the secondary metabolism, principally phenylpropanoid biosynthetic pathway which generates structurally diverse products involved in various ways in the plant defence response (Dixon & Paiva, 1995). The phenylpropanoids are derivatives of cinnamic acid which is synthesised from phenylalanine by the action of phenylalanine ammonia lyase (PAL), the entry point into the pathway (Hotter, 1997). Specific branch pathways are responsible for synthesis of more complex compounds such as flavonoids, isoflavonoids and stilbens, many of which exhibit a broad spectrum of antimicrobial properties (e.g. phytoalexins) and may play important roles as signal molecules (Dixon *et al.*, 2002). Phenylpropanoid lignin precursors are polymerized by peroxidases present in the intracellular space, leading to physical reinforcement of the plant cell wall. Further modification of mechanical properties of the cell wall is achieved during peroxidase catalysed oxidative coupling of phenolic esters into the cell wall. Deposition of lignin and other cell wall-bound phenolics has been described for many plant species in response to microbial attack (Cvikrova *et al.*, 2006; Hotter, 1997).

Overall, most information available on plant responses to pathogenic infection originates from studies on agricultural crop plants (Dangl & Jones, 2001). Very little basic molecular work on plant-pathogen interactions has been done on tree pathosystems, particularly on gymnosperms. In terms of evolution, gymnosperms and angiosperms are thought to be quite distinct groups that separated from each other several hundred million years ago (Savard *et al.*, 1994). Despite their separation, the defence strategies and mechanisms engaged by the two plant groups for resisting pathogen invasion are thought to be conserved (Pearce, 1996). However, in contrast to angiosperms, we do not have a global overview of a gymnosperm pathosystem regarding the nature, types and kinds of proteins or genes that may be involved in disease resistance.

A diverse array of phenolic compounds, including phenylpropanoids, stilbenes, flavonoids and lignans, is accumulated by conifers after *H. annosum* s.l. attack (Asiegbu *et al.*, 1998; Johansson, Lundgren & Asiegbu, 2004; Lindberg *et al.*, 1992). Pathogenesis-related (PR) proteins produced in conifer tissues in response to *H. annosum* s.l. infection include defensin SPI1 (Fossdal *et al.*, 2003) and a large number of enzymes: chitinases, glucanases (Asiegbu *et al.*, 1995; Hietala *et al.*, 2004) and extensively studied peroxidases (Asiegbu, Daniel & Johansson,

1994; Johansson, Lundgren & Asiegbu, 2004; Nagy *et al.*, 2004b). Recently, a transcriptome approach has been applied to investigate both the pathogen and the host. Fungal genes differentially expressed during contact with roots included genes encoding mitochondrial proteins, a cytochrome P450 and a vacuolar ATP synthase (Karlsson, Olson & Stenlid, 2003). Analysis of a subtractive cDNA library of Scots pine roots led to the identification of candidate genes involved in cell rescue and defence such as peroxidase, antimicrobial peptide (*SpAMP*), thaumatin, metallothionein-like protein and R gene homologue (Asiegbu *et al.*, 2003; Asiegbu, Nahalkova & Li, 2005).

Transcriptome approach and particularly microarray technology offer possibility of global analysis of gene expression which is especially useful in the field of plant defence (Reymond, 2001). So far there is no established case of a compound or pathway that is exclusively involved in pathogen defence (Somssich & Hahlbrock, 1998). It rather seems that the overall response combines all possible mechanisms that together form a large arsenal. The DNA microarrays have been successfully used to study plant development (Brinker *et al.*, 2004), stress (Kovalchuk *et al.*, 2005; Watkinson *et al.*, 2003) and defence response (Bar-Or, Kapulnik & Koltai, 2005), also in conifers (Myburg *et al.*, 2006; Ralph *et al.*, 2006a; Ralph *et al.*, 2006b). Transcriptomics can help to advance our understanding of plant-pathogen interactions. The gained knowledge would facilitate the identification of useful resistance markers necessary for molecular breeding and would also be invaluable for understanding basis for variation in natural resistance.

The goal of the study was to gain insights into molecular basis of *P. sylvestris* L.-*H. annosum* (Fr.) Bref. sensu stricto interaction. A comprehensive analysis of expression of over 2000 expressed sequence tags (ESTs) was performed at three time points (1, 5 and 15 days post inoculation) marking different stages of pathogen development: adhesion/hyphal growth, cortical invasion and vascular colonization respectively with a corresponding host responses in the form of recognition and active defence. Several pathways potentially used by conifer trees for responding to fungal infection were identified and discussed with reference to literature reports on conifer and agricultural crop pathology.

Materials and Methods

Host plant, pathogen and root inoculation

Pinus sylvestris seeds (provenance Eksjö, Sweden) were surface sterilized with 33% H₂O₂ for 15 min, rinsed in several changes of sterile distilled water, sown on 1% water agar and left to germinate under a photoperiod of 16h light at 14/8°C day/night temperature. After 14 days, the seedlings were used for inoculation. *Heterobasidion annosum* s.s. (isolate FP5, obtained from K. Korhonen, Finnish Forest Research Institute, Finland) was maintained on Hagem agar (Stenlid, 1985) at 20°C. The mycelium used for inoculation was obtained from cultures grown in liquid Hagem medium for 14 days in static conditions. The mycelium was washed with sterile water and subsequently homogenized for 60 seconds in a sterile

Waring blender. Ten seedlings of *P. sylvestris* were transferred to wet, sterile filter paper placed on 1% water agar in Petri dishes. The roots were inoculated with 1 ml of the mycelial homogenate and covered with a second set of moist sterile filter paper. The plate was sealed with parafilm and the region of the dish containing the roots was covered with aluminium foil. The seedlings were then kept under a photoperiod of 16h light at 18°C. Control plants were mock-inoculated with 1 ml sterile distilled water. The roots of 100 seedlings of either infected or control plants were harvested at 1, 5 and 15 days post inoculation (d.p.i.), ground in liquid nitrogen and stored at -80°C until RNA extraction. There were three biological replications.

Preparation of samples for scanning and transmission electron microscopy (SEM and TEM)

Five seedlings were harvested 1, 5 and 15 d.p.i. Root samples (10 mm from the tip) were excised from each plant, prefixed in 3% (v/v) glutaraldehyde, washed in phosphate buffer (3 x 10 min) and post-fixed for 3h in 1% (w/v) osmium tetroxide. After washing in distilled water (4 x 15 min), roots were dehydrated using a 10 step ethanol series (i.e 10%, 20%, 30% to 100%), then an ethanol-acetone series (3:1, 2:2, 1:3, pure acetone, 10 min each), and dried using a polaron critical point dryer. Samples were mounted on stubs using double sided adhesive tape and coated with gold using a Polaron E5000 sputter coater. Roots were observed using Hitach S-4500 SEM operated at 15 kV. Samples for TEM were prepared as previously described (Asiegbu, Daniel & Johansson, 1994).

***Pinus taeda* cDNA library construction and characteristics of analysed ESTs**

The ESTs used for this study were obtained from six cDNA libraries of *P. taeda* representing different developmental stages in wood formation (<http://biodata.ccgb.umn.edu/>) (Kirst *et al.*, 2003). The 2109 ESTs on the array were functionally annotated by reference to the *Arabidopsis thaliana* database at <http://pedant.gsf.de> and the Genbank. The best hit from the BLAST search was utilized for grouping the cDNAs into functional categories (see Stasolla *et al.*, 2003).

Microarray preparation

Probe preparation was performed in accordance with procedures published before (Kirst *et al.*, 2003; Stasolla *et al.*, 2004; Stasolla *et al.*, 2003). DNA from each of 2109 ESTs was printed onto amino-silane coated CMT-GAPS slides (Corning Inc; Corning, NY, USA) in four replications for hybridizations performed at 1 d.p.i. and in two replications at 5 and 15 d.p.i. using a Lucidea Array Spotter (Amersham Biosciences, USA). After printing, the DNA was cross linked using 250 mJ of UV-C radiation. The slides were subsequently baked at 75°C for 2 hrs, stored in slide containers in the dark at room temperature and used within 10 days.

cDNA labeling and hybridisation

Total RNA was isolated from infected and control roots of *P. sylestris* seedlings as described by Chang (1993). The cDNA was synthesised from the same amount of RNA (1 µg) using SMART™ PCR cDNA synthesis kit (Clontech, USA). The cDNA generated from infected and control roots at one time point was reciprocally labelled with Cy3 and Cy5-dUTP (Perkin Elmer, USA) using a Klenow method. Labeling, hybridization, and stringency washes followed the protocol from North Carolina State University (Brinker *et al.*, 2004); van Zyl, U.S. Provisional Patent Application Nos. 60/372,872 and 60/390,142). The experimental design involved comparison of inoculated versus un-inoculated sample at one time point: 1, 5 or 15 d.p.i. Taking into consideration dye-swaps and technical replicates, each sample was hybridized six times and there were a total of 72 data points for each gene on the array at 1 d.p.i. and 36 at 5 and 15 d.p.i. Slides were scanned with a ScanArray 4000 (GSI Lumonics, Oxnard, CA USA) and raw non-normalized intensity values were registered using Quantarray software (GSI Lumonics).

Statistical analysis

Significance in transcript abundance changes was estimated using two successive mixed models as described in Wolfinger *et al.* (2001) and Jin *et al.* (2001).

$$\text{Log}_2(Y_{ijkmg}) = L_i + T_j + D_k + LT_{ij} + LD_{ik} + TD_{jk} + S_l + B_m + SB_{lm} + SD_{lk} + BD_{mk} + \epsilon_{ijkmg} \quad (\text{M1})$$

$$R_{ijkmg} = L_{ig} + T_{jg} + D_{kg} + LT_{ijg} + LD_{ikg} + TD_{jkg} + S_{lg} + BS_{img} + SD_{lkg} + \xi_{ijkmg} \quad (\text{M2})$$

Model M1 is used to normalize all the data, and Model M2 is then fit separately to one gene at a time. Y_{ijkmg} represents the raw intensity measurement from the i^{th} cell line (batch), the j^{th} treatment, the k^{th} dye channel, the l^{th} slide, and the m^{th} block in the array for the g^{th} gene. R_{ijkmg} represents the residual computed as $\text{Log}_2(Y_{ijkmg})$ minus the fitted effects from (M1). The symbols L, T, D, S, and B represent effects of cell line, treatment, dye, slide and block effect, respectively. Double symbols represent corresponding interaction effects. The terms S, B, SB, SD, and BD in (M1) are considered to be random effects, as are terms S, BS, and SD in (M2); others are fixed effects, and ϵ and ξ are stochastic errors. All the random effect terms including the errors are assumed to be normally distributed with mean 0 and effect-specific variance components. Estimates of fold changes for each gene and their statistical significance are based on fitted values from (M2). Many transcript abundance expression changes less than two-fold were statistically significant (Jin *et al.*, 2001); however, some compression in these estimates is likely, as shown in later comparison with real-time RT-PCR. To conservatively ensure a false positive rate of 0.01, a p-value cutoff was set at the Bonferroni value of $0.01/2109 = 4.5 \times 10^{-6}$, as suggested by Wolfinger *et al.* (2001).

Real-time quantitative RT-PCR analysis of gene transcription

Verification of expression of selected genes was performed using real-time quantitative RT-PCR. Total RNA was extracted from seedlings infected

independently from the microarray experiment and there were three biological replicates. The RNA (2 µg) was digested with deoxyribonuclease I (Sigma, Sweden) according to manufacturer's instructions and further quantified using Quant-iT RiboGreen RNA Assay Kit (Molecular Probes, Invitrogen, Sweden). Equal amount of RNA (1 µg) was reverse transcribed with M-MLV reverse transcriptase (Invitrogen, Sweden) following manufacturer's instructions. As positive control of the reverse transcription, 5000 copies of kanamycin mRNA (Promega) were added to the reaction mixture. Specific primer pairs (see Supplementary Table S2) were designed against each gene with amplicons ranging from 54 to 147 bp. The relative transcript abundance was detected by the ABI Prism 7700 Sequence Detection System (Perkin-Elmer Applied Biosystems, Sweden) using SYBR Green PCR Master Mix (Applied Biosystems) according to manufacturer's recommendations. Transcript levels were calculated from three technical replicates using the standard curve method (User Bulletin #2, ABI Prism 7700 Sequence Detection System, Applied Biosystems). For preparation of the standard curve, plasmids of interest were extracted with QIAprep[®] Spin Miniprep kit (Qiagen). The plasmid DNA concentration was determined using Quant-iT PicoGreen dsDNA Kit (Molecular Probes, Invitrogen, Sweden). A serial dilution of each plasmid was prepared, including 10⁶, 10⁵, 10⁴, 10³, 10² copies/µl and real-time RT-PCR was performed. The absolute quantity of the product in each sample was calculated from the standard curves and was normalized against total amount of RNA as described previously (Hashimoto, Beadles-Bohling & Wiren, 2004; Silberbach *et al.*, 2005). The correction for reverse transcription reaction based on kanamycin amplification was included into calculations.

Cellular localization of antimicrobial peptide (AMP)

The AMP peptide sequence used for raising polyclonal antibody corresponded to amino acids within the conserved region of the gene (Asiegbu *et al.*, 2003). The immunization procedure was performed with the peptide coupled to ova-albumin as a carrier (www.peptron.com). Polyclonal antibody was raised against the synthetic peptide using rabbits at the Statens Veterinärmedicinska Anstalt (SVA, Uppsala, Sweden). The antibody was shown to cross react with proteins from root, stem and needle extracts (data not shown). The antiserum was used to localize sites of accumulation of AMP within *H. annosum* infected pine roots and uninfected control at 15 d.p.i. The procedures for embedding, tissue fixing and immunocytochemical labelling were previously described (Asiegbu, Daniel & Johansson, 1994) except that gelatine was used as blocking agent instead of Bovine serum albumin (BSA). The sections were examined using a Philips EM201 transmission electron microscope operated at 60kV.

Sequences analysis

Genes identified as differentially expressed during infection of *P. sylvestris* roots with *H. annosum* were subjected to contig analysis with SeqMan (MegAlign™ expert sequence analysis software, version 5.05). Prediction of signal peptide cleavage sites and subcellular location were done with aid of tools available at

ExpASy Proteomics Server (<http://www.expasy.org/tools/>): SignalP 3.0 (Bendtsen *et al.*, 2004) and WoLF PSORT (Horton *et al.*, 2006), respectively.

Results

Infection development

Pinus sylvestris seedling roots were inoculated with homogenized mycelia of *H. annosum*. Adhesion of hyphal material was followed by appressorium formation and hyphal penetration one day post inoculation (d.p.i.) (Figure 1a-d). At this time no visible symptoms of the infection such as necrotic browning were observed on the roots. Roots which were exposed for longer period (5-15 days) developed typical necrotic browning. By 15 d.p.i, the root surface was covered with extensive network of hyphae (Figure 1e) compared to the un-inoculated control root (Figure 1f) and approximately 30% of the seedlings exhibited loss of root turgor. Transmission electron micrographs revealed massive invasion of the root tissues by the fungal hyphae actively degrading the host cell wall (Figure 2b, c, d). It also showed accumulation of electron dense materials, probably phenolics (Figure 2a, c) and mechanical defence reactions including cell wall thickening as a result of lignification (see below) (Figure 2c).

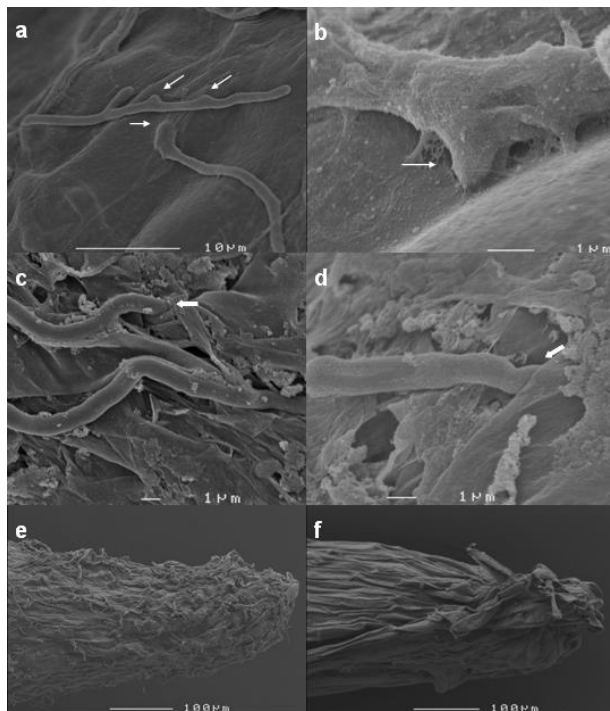


Fig. 1. Scanning electron microscope (SEM) photographs of inoculated *P. sylvestris* roots showing development of infection with *H. annosum*: a, b) development of infection structures (appressoria - arrows); c, d) penetration of the root (block arrow); e) extent of root colonisation by the fungal hyphae at 15 d.p.i compared with f) control root. Bar represents 1, 10 or 100 μm .

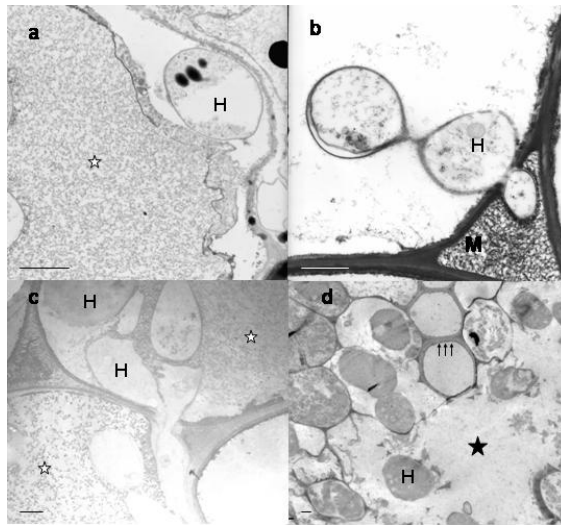


Fig. 2. Transmission electron microscope (TEM) photographs of inoculated *P. sylvestris* roots showing development of infection with *H. annosum*: a) shrinkage of plant cytoplasm avoiding contact with the hyphae (H) surrounded by electron dense material, probably phenolics (white star); b) fungal hyphae breaching the cell wall (M- middle lamella cell corner region); c) progressing colonisation of the plant tissues by the fungal hyphae; d) advanced root tissue degradation 15 d.p.i. (star) and example of structural defence in the form of cell wall thickening (arrow). Bar represents 1 μ m.

Sensitivity of the microarray experiment and statistical analysis

To analyse changes in gene transcript levels in *P. sylvestris* root tissues infected by *H. annosum*, a cDNA microarray containing 2109 ESTs from *P. taeda* was used. Due to amplification of RNA prior to microarray hybridizations low fold changes were generally observed. However, by applying a stringent statistical methodology using 2-mixed model analysis (Wolfinger *et al.*, 2001), it was possible to declare genes with fold changes as low as 1.3 to be statistical significant. This was feasible due to high number of biological and technical replications which were as high as 36 – 72 per gene. Application of a cut-off value of 1.3 average fold change in at least two out of three biological replicates, led to identification of over 500 genes differentially expressed with a total of 43, 165 and 421 genes at 1, 5 and 15 d.p.i., respectively (see Supplementary Table S1). We decided to increase the stringency to an average fold change of 1.4 in all three biological replicates which led to a manageable number of genes that are discussed below.

Transcript profiling of differentially expressed *P. sylvestris* genes during infection with *H. annosum*

Mixed model analysis identified 179 ESTs differentially expressed at 1, 5 or 15 d.p.i. with a fold change greater than 1.4 (for genes up-regulated) or below -1.4 (for genes down-regulated) (Table 1). Contig analysis of those sequences showed that 15 contigs were represented by two ESTs each. The fold changes of both ESTs constituting each contig had similar fold change values (Table 1).

Ultimately, there were 164 unique genes differentially expressed by *P. sylvestris* in response to *H. annosum*. Pairwise comparison of the infected seedlings versus un-inoculated controls distinguished a total of 5, 24 and 90 ESTs that showed significant increase in transcript levels at 1, 5 and 15 d.p.i., respectively. Eighteen ESTs were overlapping between 5 and 15 d.p.i. and among those, three were common for all the three time-points: thaumatin and two ESTs belonging to the same contig, coding for peroxidase (Table 1). The number of the ESTs with decreased transcript levels was 0, 6 and 80 at 1, 5 and 15 d.p.i., respectively, and five genes were commonly down-regulated at both 5 and 15 d.p.i. (Table 1). In general, the total number of genes differentially expressed during the infection increased over time.

Real-time RT-PCR validation of expression of selected genes

To evaluate the validity of the microarray results, the expression patterns of fourteen genes were further examined by real-time RT-PCR. The fold changes determined by real-time RT-PCR were usually higher but otherwise consistent with the microarray data (Table 2). For example, in the array, a fold change of -1.7 was recorded for xyloglucan endotransglycosylase with a corresponding value of -15.4 in the real-time RT-PCR. Similarly, peroxidase with a fold change value of 3.4 in the array at 15 d.p.i. had a value of 24.8 in the real-time RT-PCR experiment. However, fold changes of thioredoxin, a gene identified in the array as down-regulated, was reproduced by the real-time RT-PCR with good precision (Table 2). S-adenosylmethionine synthase expected not to be differentially expressed at 1 d.p.i. was confirmed by the real-time RT-PCR to have stable transcript level. Also, regulation of genes identified as differentially expressed with lower stringency (average fold change 1.3 in at least two out of three replicates; Supplementary Table S1) was confirmed. The distribution of copy numbers of the biological replicates in the control and infected pine roots is presented in Supplementary materials (Figure S1).

Functional classification of genes differentially expressed

The gene expression in major functional categories is shown in figures 3a-b as percentage of all the genes belonging to the given category present on the array. The most prevalent of the ESTs up-regulated in response to the pathogen invasion belonged to the functional group of primary and secondary metabolism (Figure 3a). Within the primary metabolism, genes encoding enzymes involved in two major biochemical pathways were identified: shikimate pathway (3-deoxy-D-arabino-heptulosonate-7-phosphate synthase and prephenate dehydratase) and methionine synthesis (adenosylhomocysteinase, methionine synthase and adenosylmethionine synthetase) (Figure 4). The shikimate pathway provides carbon influx into the phenylpropanoid pathway (stilbene, flavonoids and lignin biosynthesis) with phenylalanine ammonia lyase as an entry point (Figure 4). The genes coding for enzymes in the described pathways had increased transcript levels at either 5, 15 d.p.i. or both time-points, except the peroxidase gene transcripts which were up-regulated at all three time points (Figure 4). Several other genes with functions related to cell, tissue and organ differentiation and

system regulation of interaction with environment were up-regulated. The group with the next most abundant transcripts encoded proteins involved in energy acquisition, mainly in respiration and photosynthesis (Table 1). A number of up-regulated genes was related to cell rescue and defence and included antimicrobial peptide, chitinase, metallothionein and thaumatin (Table 1). Apart from genes encoding proteins with defined functions, a high number of genes with increased transcription coded for unclassified and proteins with unknown function. Overall, the general trend of increase in the number of differentially expressed genes over time was particularly visible within the following functional categories: metabolism, cell rescue and defence and unknown.

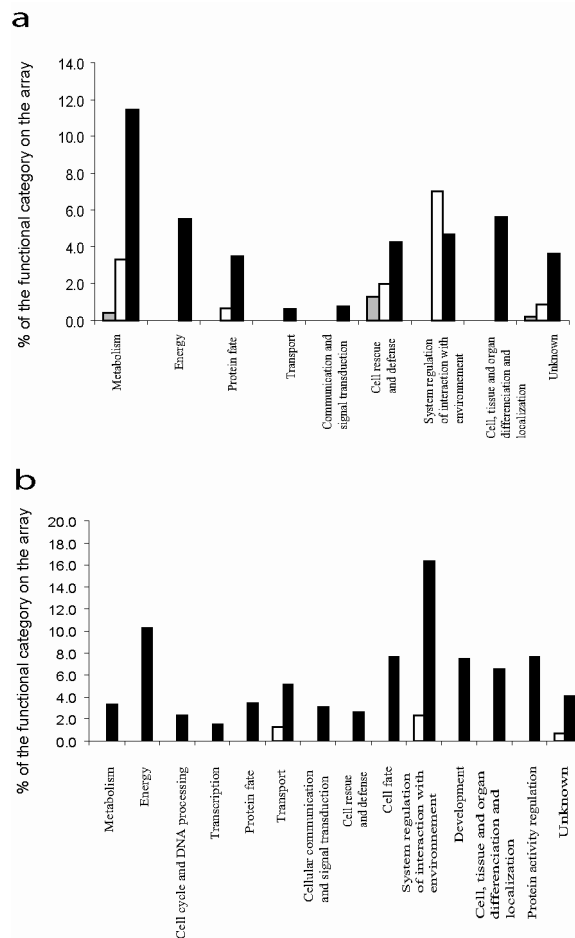


Fig. 3. The percentage of genes differentially expressed by *P. sylvestris* in response to *H. annosum* infection relative to functional classes on the array; a) genes up-regulated at 1 (grey), 5 (white) and 15 d.p.i (black); b) genes down-regulated at 5 (white) and 15 d.p.i (black) (at 1 d.p.i. there was no gene with transcript level significantly lower in the infected roots than in the control).

Most of the down-regulated genes encoded proteins with functions important in regulation of interaction with environment (auxin or gibberellin regulated, water stress inducible) or energy acquisition (particularly photosynthesis related) (Figure

3b, Table 1). A number of other down-regulated genes had functions related to protein activity regulation and development. Two interesting genes, cyclin dependent kinase and BAX inhibitor, with functions related to cell cycle and cell fate, respectively, were found to be down regulated. Interestingly, some of the down-regulated genes were those with functions vital for cell rescue and defence, like chitinase or NBS/LRR disease resistance protein (Table 1). Furthermore, a large number of genes encoding unclassified and unknown proteins also had decreased transcript levels. A number of genes (e.g. chitinase, peroxidase and lipase) were found to be regulated in opposite way (Table 1). Contig analysis indicated that those genes belonged to separate contigs.

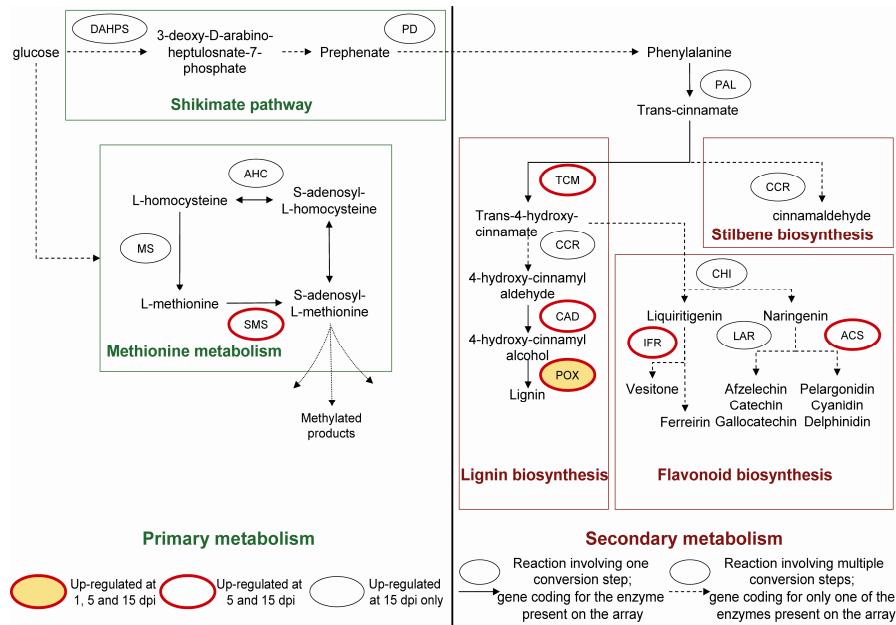


Fig. 4. *Heterobasidion annosum*-induced genes coding for enzymes involved in primary and secondary metabolism. Abbreviations: ACS - anthocyanidin synthase (E.C. 1.14.11.19), AHC - adenosylhomocysteinase (E.C. 3.3.1.1), CAD - cinnamyl alcohol dehydrogenase (E.C. 1.1.1.195), CCR - cinnamoyl CoA reductase (E.C. 1.2.1.44), CHI - chalcone-flavone isomerase (E.C. 5.5.1.6), DAHPS - 3-deoxy-D-arabino-heptulosonate-7-phosphate synthase (E.C. 4.1.2.15), IFR - isovlavone reductase (E.C. 1.3.1.45), LAR - leucoanthocyanidin reductase (E.C. 1.17.1.3), MS - methionine synthase (E.C. 2.1.1.13), PAL - phenylalanine ammonia lyase (E.C. 4.3.1.5), PD - prephenate dehydratase (E.C. 4.2.1.51), POX - peroxidase (E.C. 1.11.1.7), SMS - adenosylmethionine synthetase (E.C. 2.5.1.6), TCM - trans-cinnamate-4-monooxygenase (E.C. 1.14.13.11).

General patterns of gene regulation during *H. annosum* infection

To group genes with similar regulation patterns during *P. sylvestris* infection with *H. annosum*, a hierarchical clustering analysis was performed on 179 ESTs whose expression changed substantially in response to the pathogen (Figure 5). All the differentially expressed genes were grouped into eight regulatory patterns. (Figure 5, Table 1). Cluster 1 included genes down-regulated weakly at 1 d.p.i. and more strongly at 5 and 15 d.p.i. (e.g. lipase, BAX inhibitor and cyclin dependent

kinase). Cluster 2 contained genes with only small expression changes as compared to the un-inoculated seedlings at the early and intermediate time point and up-regulated at 15 d.p.i (e.g. 26S proteasome subunit, leucoanthocyanidin dioxygenase).

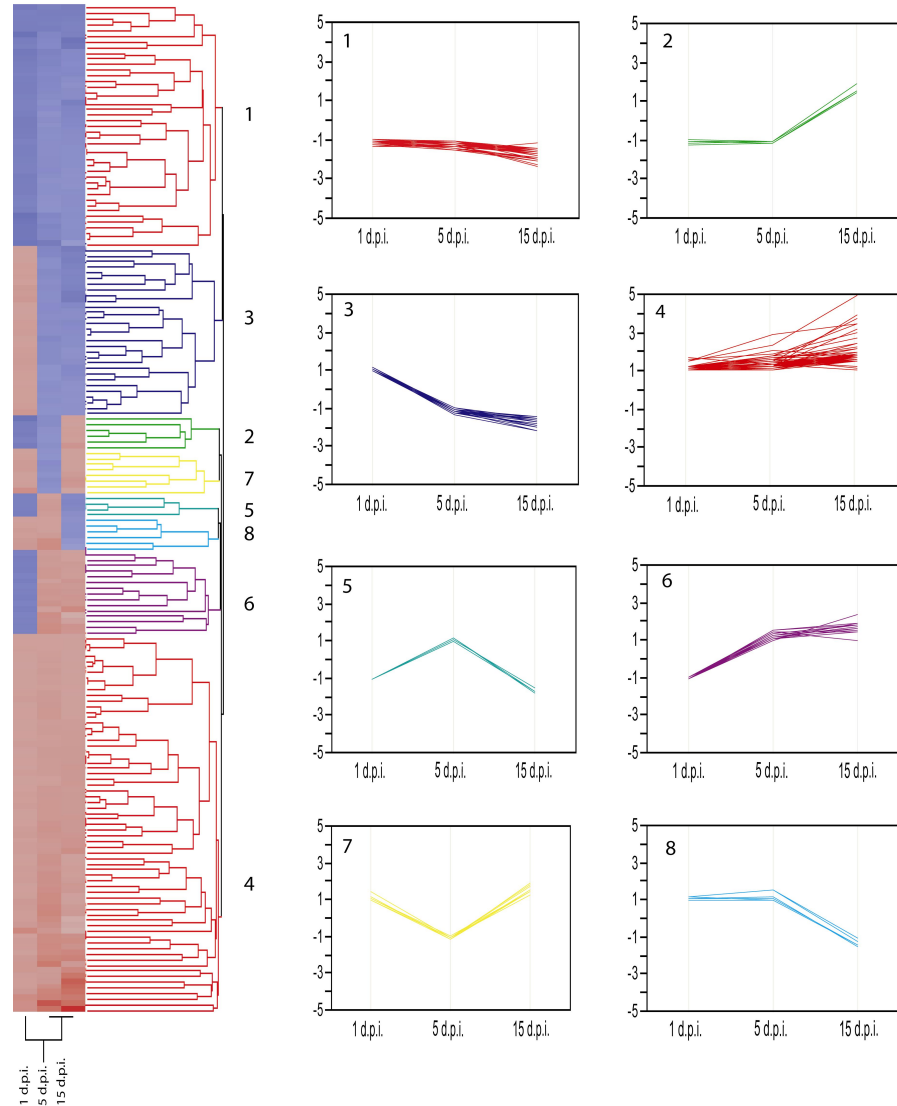


Fig. 5. Hierarchical clustering illustrating groups of *P. sylvestris* genes coordinatively expressed in response to *H. annosum* infection at 1, 5 and 15 d.p.i. Each column corresponds to a time-point (1, 5 or 15 d.p.i.) and each row illustrates expression profile of each of 179 differentially expressed ESTs over the three time points. For each gene, the fold change of mRNA level in inoculated versus corresponding control tissues is represented by red-blue colour, meaning up-regulation and down-regulation. All the differentially expressed ESTs were divided into 8 regulatory patterns, indicated by the numbers 1-8.

Genes in cluster 3 were weakly up-regulated at the beginning of the infection process and then down-regulated at the intermediate and late time-point. A significant number of genes in cluster 3 was represented by those coding for photosynthesis related proteins (Table 1). The highest number of genes grouped in cluster 4 with expression levels higher than in the control at all time points. Among them were enzymes important in primary and secondary metabolism (e.g. phenylalanine ammonia-lyase, peroxidase). Cluster 5 consisted of genes not differentially expressed at the early stage of infection, weakly up-regulated at the intermediate one and highly down-regulated at the last time-point (Figure 5). There were four genes in this group: xyloglucan endo-transglycosylase, trans-cinnamate 4-hydroxylase, NBS/LRR disease resistance and thiamine biosynthetic enzyme. Genes grouped in cluster 6 had expression levels similar to the control seedlings at 1 d.p.i. and were up-regulated at 5 and 15 d.p.i. (e.g. defence-related genes coding for heat shock protein, thioredoxin and cinnamyl alcohol dehydrogenase). Cluster 7 consisted of genes weakly up regulated at the beginning of the infection with *H annosum*, weakly down-regulated on the intermediate stage and highly up-regulated in the late phase (e.g. cinnamoyl CoA reductase). Finally, cluster 8 contained genes not differentially expressed at 1 and 5 d.p.i. and down-regulated at the last time point, like glutathione-S-transferase (Figure 5).

Peroxidase sequence analysis

The microarray contained six ascorbate peroxidases, one glutathione peroxidase and seven class III peroxidases. Two ESTs identified by the microarray analysis of *P. sylvestris* transcriptome upon infection with *H annosum* to be up-regulated at 1, 5 and 15 d.p.i., coded for one class III plant peroxidase. Contig analysis of the ESTs in the *P. taeda* database coding for peroxidase (http://biodata.ccgb.umn.edu/doepine/contig_dir20/, contigs 6216 and 6336) detected a consensus sequence of 1172 bp. The sequence was found to contain an open reading frame encoding a polypeptide of 351-amino acids. The gene had a 5' untranslated region of 54 bp and a 3' untranslated region 116 bp long. Sequence analysis predicted that the protein was a secretory one and that it contained a signal peptide of 16 amino acids.

Cellular localisation of antimicrobial peptide (AMP)

Both microarray and real-time RT-PCR analyses revealed that *P. sylvestris* root tissues in response to infection with pathogen *H. annosum* had elevated transcript levels of genes coding for antimicrobial peptide (AMP). To confirm accumulation of the protein and determine its cellular localisation at 15 d.p.i., an immunocytochemical study was performed using specific antibody. The amount of AMP increased significantly in the cells of infected root (Figure 6). The proteins were found mostly in the cell wall region, particularly middle lamellar cell corner region (Figure 6).

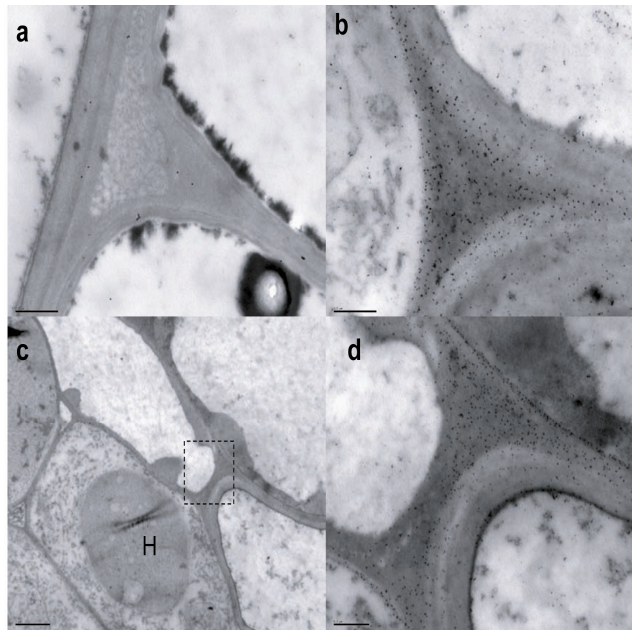


Fig. 6. Transmission electron microscope photographs of *P. sylvestris* un-infected and *H. annosum* infected roots showing immuno-localisation of antimicrobial peptide (AMP) at 15 d.p.i.: a) cell wall region in the control root and corresponding region in the b) infected root illustrate increased accumulation of the AMP (black dots - gold-labelled secondary antibodies); c) hyphae (H) infecting plant cell; neighbouring cell wall region (dashed square) is enlarged in d). Bar represents 0.2 μ m (a, b, d) and 1 μ m (c).

Discussion

While knowledge about regulation of defence and resistance in agricultural and horticultural crops is well established, the nature of defence response and disease resistance in pines and other gymnosperms remains largely unexplained (Anderson, Thatcher & Singh, 2005; Franceschi *et al.*, 2005; Somssich & Hahlbrock, 1998). This is due to lack of host material with defined genetic background: although clonal systems and transformation method are available, they remain a slow and tedious process (Elfstrand *et al.*, 2001; Hogberg *et al.*, 1998). Moreover, the long life cycle and large size of mature trees make working with those plants inherently difficult. In an effort to develop a working model system for conifer-pathogen interactions, we have used *P. sylvestris* seedlings infected with *H. annosum*, fungus able to infect conifers of all ages (Asiegbu, Daniel & Johansson, 1994; Li & Asiegbu, 2004). The process of infection in this system is well documented (Asiegbu, Adomas & Stenlid, 2005). Previous studies have shown that suberized and non-suberized roots respond in a similar way to the pathogen infection (Asiegbu, Daniel & Johansson, 1994; Johansson, Lundgren & Asiegbu, 1994). Accordingly, *P. sylvestris* seedlings-*H. annosum*

pathosystem appears to be a good model to study pine defence mechanisms in terms of size, time and correlation with more advanced plant developmental stages.

The high correlation of transcript level for the same tissues between *P. sylvestris* and *P. taeda* ($r=0.93$) (van Zyl *et al.*, 2002) permits differential screening to be done using the loblolly pine arrays with RNA obtained from Scots pine. In the present study, a heterologous array consisting of 2109 ESTs was used to document molecular events following *P. sylvestris* infection with a necrotrophic fungal pathogen *H. annosum* at 1, 5 and 15 d.p.i. Mixed model analysis identified 179 differentially expressed ESTs and noted a general tendency of increase over time in number of genes differentially regulated. The delay (5-15 d.p.i.) before detection of substantial plant response contrasts with prompt hypersensitive reaction related symptoms usually visible within hours or even seconds after infection in angiosperms (Heath, 2000). Gymnosperm pathosystems tend to respond in a slower manner to pathogen attack (Hietala *et al.*, 2004; Nagy *et al.*, 2004a; Pearce, 1996). Although a number of proteins (*P. nigra* chitin binding lectin, PNL) and genes (*avr9/cf-9* rapidly elicited-homolog [PsACRE], leucine rich repeat [LRR] R-gene homolog) with roles in recognition and signal transduction has recently been described in *P. sylvestris*-*H. annosum* pathosystem, gene-for-gene interactions have not been documented (Asiegbu, Adomas & Stenlid, 2005). The small number of genes differentially expressed at the early stage of interaction may reflect a lack of information a plant possesses about the nature of the attack during initial phase of infection (Franceschi *et al.*, 2005). It is also possible that the pathogen has evolved a strategy to mask detection by the conifer root. For example, masking chitin and glucan molecules that may act as potential elicitors could delay plant responses until the pathogen has established itself in the host. Furthermore, the histochemical observations confirmed that pre-penetration events occurred in our model system at 1–2 d.p.i., penetration into epidermis and cortex at 3-5 d.p.i. and into endodermis and vascular region at 9–15 d.p.i. Therefore, it was not surprising that increased gene transcripts were recorded in parallel to severity of damage to host tissues during intracellular colonization. In any case, in the absence of precise recognition of the aggressor, general broad-based defences would be important.

In our experiment, at 1 d.p.i. two genes coding for proteins with antimicrobial properties were found to be significantly up-regulated: thaumatin and antimicrobial peptide (AMP). Thaumatin-like proteins exhibit antifungal activity *in vitro* and are thought to create transmembrane pores, thus permeabilizing fungal hyphae (Li & Asiegbu, 2004; Monteiro *et al.*, 2003). Antimicrobial peptides have been detected in a wide variety of agricultural plant species and have been implicated in resistance of such plants to microbial infections (Broekaert *et al.*, 1997). Similar role has been suggested for conifer defensins (Fossdal *et al.*, 2003; Pervieux *et al.*, 2004). A cDNA encoding pine antimicrobial peptide (SpAMP) was the most abundant transcript in subtractive cDNA library from *P. sylvestris* roots infected with *H. annosum* (Asiegbu, Nahalkova & Li, 2005). The mode of action of SpAMP and its counterpart from *Macadamia integrifolia* (MiAMP1) remains unknown, even though it has been shown that their structural homolog, yeast killer toxin WmKT interferes with cell wall biosynthesis by inhibiting β -1,3-

glucan synthase (Asiegbu *et al.*, 2003; Stephens *et al.*, 2005; Yabe *et al.*, 1996). Immunocytochemical localization of AMP revealed substantial accumulation of the peptide in the cell wall region at 15 d.p.i. (Figure 6). Abundance of the antimicrobial peptide on the cell surface may indicate a direct role of AMP in defence against invading fungal hyphae. Although at higher statistical stringency, the array showed significant up-regulation of AMP gene only at 1 d.p.i., northern blot analysis (Asiegbu *et al.*, 2003), real-time RT-PCR (Table 2) and immunocytochemistry (Figure 6) demonstrated accumulation of the transcript and the protein at 1 to 15 d.p.i. The higher expression ratios of AMP determined by real-time RT-PCR than ratios determined by the array suggest that the real-time RT-PCR is more sensitive technique than the transcript profiling using microarray (Manthey *et al.*, 2004; Yuen *et al.*, 2002).

Many of the genes induced during more advanced stages of *H. annosum* infection were involved in secondary metabolism (Figure 4). Numerous chemicals are produced by enzymes active in phenylpropanoid pathway, starting with phenylalanine ammonia lyase and branching into lignin, stilbene and flavonoid biosynthesis (Dixon & Paiva, 1995). Lignin and suberin are two groups of compounds which strengthen the cell wall and may block penetration at the sites of infection. Lignin production is catalysed by laccase and peroxidase controlling polymerisation of monolignols (Whetten, MacKay & Sederoff 1998). Class III secretory peroxidases have been associated with plant defence and resistance, particularly with lignin and suberin synthesis, but also with cross-linking phenolic compounds into papillae and production of toxic compounds (Asiegbu, Daniel & Johansson, 1994; Fossdal, Sharma & Lonneborg, 2003; Takahama & Oniki, 2000). Sequence analysis of the peroxidase gene up-regulated during whole infection process, detected a 16-amino acids long signal peptide and predicted an extracellular localisation of the mature protein which indicates it might be associated with the cell wall. Increased lignin synthesis and deposition leading to cell wall thickening have been recorded during pathogen attack (Bonello & Blodgett, 2003) and is considered to be main mechanical defence mechanism. Stilbenes are described as phytoalexin-like compounds or phytoanticipins, because they are strongly antimicrobial *in vitro* but are often present constitutively (Bonello & Blodgett, 2003; Chiron *et al.*, 2000). Flavonoids are known for their antioxidant properties (Takahama & Oniki, 2000) and could be involved in limiting damages caused by peroxidase mediated production of toxic radicals. It should be however noted that different species produce very different phenylpropanoid compounds using the same conserved classes of enzymes (Dixon *et al.*, 2002; Dixon & Paiva, 1995). Moreover, those enzymes are coded by multigene families with different family members proposed to be independently regulated (Dixon *et al.*, 2002). This hypothesis seems to be confirmed by our study: trans-cinnamate-4-hydroxylase and peroxidase were represented in the array by at least two ESTs regulated in an opposite way (up- and down-) (Table 1).

Successful resistance to pathogens depends not only on genetics - ability to produce certain antimicrobial compounds; but also on physiology - ability to compensate high costs of investing into constitutive defence mechanisms and later on into the inducible ones. The metabolic shift into increased production of

secondary compounds initiated at 5 d.p.i. was intensified at 15 d.p.i. and completed by induction of enzymes involved in primary metabolism. Genes encoding enzymes active in methionine metabolism had elevated transcripts levels (Figure 4), possibly to provide activated methyl groups for production of defence-related compounds (Somssich & Hahlbrock, 1998). Similarly, shikimate pathway was induced to provide additional flux of carbon into the secondary metabolism. Also, an up-regulation was observed among genes coding for proteins with functions related to energy acquisition.

One of the first macroscopically visible symptoms of pathogen invasion was necrotic browning reaction. As documented by transmission electron microscopy (Fig 2d), at 15 d.p.i. an extensive degradation of root tissues took place and a decrease in number of living cells occurred (Adomas et al., unpublished). A question arises whether it was solely due to the necrotrophic activity of the pathogen or whether host controlled programmed cell death (PCD) was engaged. Occurrence of several hallmarks of PCD indicates active role of the plant, although induction of the process by the pathogen can not be ruled out. Primarily, BAX inhibitor, a membrane protein that protects cells from induction of cell death (Huckelhoven, Dechert & Kogel, 2003) was down-regulated. Other PCD related genes differentially expressed during *H. annosum* infection included caspase-like protease (CLP) (gene ID ST06G07, see supplementary material) and lipases (Karonen et al., 2004). Also, a cyclin dependent kinase was down-regulated pointing towards shutting down of the cell cycle. Unfortunately, host controlled cell death can only prevent the growth of biotrophic pathogens but not necrotrophs like *H. annosum* (Karonen et al., 2004; Morel & Dangl, 1997). Since PCD is connected with production of reactive oxygen species, it could lead to uncontrolled damages at the tissue level (Morel & Dangl, 1997). Potential protecting mechanisms include anti-oxidants, like glutathione-S-transferase, metallothionein and thioredoxin up-regulated in our system, or flavonoid compounds. Induction of genes implicated in oxidative processes seems to be a common feature of conifer response to root pathogens like *H. annosum* or *Rhizoctonia* sp. (Johnk et al., 2005) and insects (Ralph et al., 2006b).

The full extent of the overall reprogramming of the infected plant functioning comprises not only positive but also negative regulatory mechanisms. The significance of gene repression during pathogen defence is probably associated with the down-regulation of all non-essential cellular activities and mobilization of the gained resources to cope with the challenge (Somssich & Hahlbrock, 1998). Interestingly, in the functional group of energy acquisition, many down-regulated genes encoded photosynthesis related proteins. Significance of photosynthesis associated transcripts in the roots could be explained by presence of proplastids.

Of the genes identified as significantly differentially expressed, 35 were categorized as having no similarities to sequences in the public database or with unknown function. These sequences may represent novel pine genes with roles in defence and disease progression.

Large scale analysis of gene expression facilitates comparison of plant reaction to different forms of stress. Recently, Ralph et al. (2006b) have used microarray technology to study spruce response to wounding and insect attack and found a

considerable overlap among differentially expressed gene sets from these treatments. Functional classification of those genes revealed down-regulation of photosynthesis related transcripts and induction of genes with role in oxidative processes and in secondary metabolism, including phenylpropanoid pathway, as found in our study. The similarity in response to wounding, insects or fungal attack may suggest conservation in conifer defence to stress.

Technically, microarray proved to be a powerful method to elucidate molecular defence mechanisms mounted by pine in response to pathogen infection. Reproducibility of the hybridization efficiency was confirmed by fold change values exhibited by ESTs belonging to the same contig (Table 1). Real-time RT-PCR verified differential expression of selected genes, although the documented fold changes were generally higher than on the array. Systemic bias of microarray technique has been reported previously (Yuen *et al.*, 2002). The difference in the results between the microarray and real-time RT-PCR, considered to be more gene-specific, could be due to cross-hybridization occurring during array hybridization between members of gene families (Chuaqui *et al.*, 2002). Besides, as there is a threshold that defines a minimum sample concentration that must be applied in a given experiment, amplification of RNA isolated from the plant material was necessary. SMARTTM PCR is a highly efficient method for exponentially amplifying RNA but the nonlinear amplification results in a target in which sequence representation is slightly skewed compared with the original mRNA pool (Puskas *et al.*, 2002; Wadenback *et al.*, 2005). This could have enlarged the differences between fold changes detected in transcript levels by microarray and real-time RT-PCR. However, other authors showed that the amplified material faithfully represents the starting mRNA population (Petalidis *et al.*, 2003; Seth *et al.*, 2003; Wilhelm *et al.*, 2006). Application of SMARTTM PCR in our experiment has probably contributed to lowering fold change values detected by the microarray. Overall, while real-time RT-PCR seems to be a more sensitive method, microarray gives a possibility of assessing changes in global expression profile and identification of novel biochemical and metabolic pathways relevant in the defence of conifer trees against pathogens.

In summary, the microarray profiling of *P. sylvestris* response to infection with fungal pathogen *H. annosum* revealed multiple overlapping strategies employed for defence purposes. Production of pathogenesis-related enzymes and antimicrobial proteins (chitinase, thaumatin, antimicrobial peptide) was supplemented by a major shift in primary and secondary metabolism. A wide array of oxidative stress protecting mechanisms was documented, possibly related to the programmed cell death. The similarity in expression profiling pattern observed in this pathosystem to those documented in crop pathology suggests that both angiosperms and gymnosperms might use similar genetic programs for responding to invasive growth of microbial pathogens. The differences in response of the two plant groups might hinge on the spatial and temporal pattern of the gene regulation. Future studies aimed at genes involved in signalling pathways would further help to elucidate our understanding of defence mechanisms in gymnosperms. Knowledge of how the defence mechanisms are regulated and maintained over long time and large physical distances in trees as compared to

short-lived annual and crop plants could be of potential ecological and biotechnological significance.

Acknowledgements

This work was supported by grants from the Swedish Research Council for Environment, Agricultural Sciences and Spatial Planning (FORMAS), the Swedish Science Research Council (VR), Carl Tryggers Stiftelse (CTS) and by the Swedish Organization for International Co-operation in Research and Higher Education (STINT).

References

- Anderson, J. P., Thatcher, L. F. & Singh, K. B. 2005. Plant defence responses: conservation between models and crops. *Functional Plant Biology* 32, 21-34.
- Asiegbu, F. O., Adomas, A. & Stenlid, J. 2005. Conifer root and butt rot caused by *Heterobasidion annosum* (Fr.) Bref. s.l. *Molecular Plant Pathology* 6, 395-409.
- Asiegbu, F. O., Choi, W. B., Li, G. S., Nahalkova, J. & Dean, R. A. 2003. Isolation of a novel antimicrobial peptide gene (Sp-AMP) homologue from *Pinus sylvestris* (Scots pine) following infection with the root rot fungus *Heterobasidion annosum*. *FEMS Microbiology Letters* 228, 27-31.
- Asiegbu, F. O., Daniel, G. & Johansson, M. 1994. Defense related reactions of seedling roots of Norway spruce to infection by *Heterobasidion annosum* (Fr.) Bref. *Physiological and Molecular Plant Pathology* 45, 1-19.
- Asiegbu, F. O., Denekamp, M., Daniel, G. & Johansson, M. 1995. Immunocytochemical localization of pathogenesis-related proteins in roots of Norway spruce infected with *Heterobasidion annosum*. *European Journal of Forest Pathology* 25, 169-178.
- Asiegbu, F. O., Johansson, M., Woodward, S. & Hüttermann, A. 1998. In *Heterobasidion annosum: Biology, Ecology, Impact and Control*. (Eds, Woodward, S., Stenlid, J., Karjalainen, R. & Hüttermann, A.) CAB International, London.
- Asiegbu, F. O., Nahalkova, J. & Li, G. 2005. Pathogen-inducible cDNAs from the interactions of the root rot fungus *Heterobasidion annosum* with Scots pine (*Pinus sylvestris* L.). *Plant Science* 168, 365-372.
- Bar-Or, C., Kapulnik, Y. & Koltai, H. 2005. A broad characterization of the transcriptional profile of the compatible tomato response to the plant parasitic root knot nematode *Meloidogyne javanica*. *European Journal of Plant Pathology* 111, 181-192.
- Bendtsen, J. D., Nielsen, H., von Heijne, G. & Brunak, S. 2004. Improved prediction of signal peptides: SignalP 3.0. *Journal of Molecular Biology* 340, 783-795.
- Bonello, P. & Blodgett, J. T. 2003. *Pinus nigra-Sphaeropsis sapinea* as a model pathosystem to investigate local and systemic effects of fungal infection of pines. *Physiological and Molecular Plant Pathology* 63, 249-261.
- Brinker, M., van Zyl, L., Liu, W. B., Craig, D., Sederoff, R. R., Clapham, D. H. & von Arnold, S. 2004. Microarray analyses of gene expression during adventitious root development in *Pinus contorta*. *Plant Physiology* 135, 1526-1539.
- Broekaert, W. F., Cammue, B. P. A., DeBolle, M. F. C., Thevissen, K., DeSamblanx, G. W. & Osborn, R. W. 1997. Antimicrobial peptides from plants. *Critical Reviews in Plant Sciences* 16, 297-323.

- Chang, S., Puryear, J. & Cairney, J. 1993. A simple and efficient method for isolating RNA from pine trees. *Plant Molecular Biology Reporter* 11, 113-116.
- Chiron, H., Drouet, A., Lieutier, F., Payer, H. D., Ernst, D. & Sandermann, H. 2000. Gene induction of stilbene biosynthesis in Scots pine in response to ozone treatment, wounding, and fungal infection. *Plant Physiology* 124, 865-872.
- Chuaqui, R. F., Bonner, R. F., Best, C. J. M., Gillespie, J. W., Flaig, M. J., Hewitt, S. M., Phillips, J. L., Krizman, D. B., Tangrea, M. A., Ahram, M., Linehan, W. M., Knezevic, V. & Emmert-Buck, M. R. 2002. Post-analysis follow-up and validation of microarray experiments. *Nature Genetics* 32, 509-514.
- Cvikrova, M., Mala, J., Hrubcova, M. & Eder, J. 2006. Soluble and cell wall-bound phenolics and lignin in *Ascochyta blight* infected Norway spruces. *Plant Science* 170, 563-570.
- Dangl, J. L. & Jones, J. D. G. 2001. Plant pathogens and integrated defence responses to infection. *Nature* 411, 826-833.
- Dixon, R. A., Achnine, L., Kota, P., Liu, C.-J., Reddy, M. S. S. & Wang, L. 2002. The phenylpropanoid pathway and plant defence - a genomics perspective. *Molecular Plant Pathology* 3, 371-390.
- Dixon, R. A. & Paiva, N. L. 1995. Stress-induced phenylpropanoid metabolism. *Plant Cell* 7, 1085-1097.
- Elfstrand, M., Fossdal, C. G., Swedjemark, G., Clapham, D., Olsson, O., Sitbon, F., Sharma, P., Lonneborg, A. & von Arnold, S. 2001. Identification of candidate genes for use in molecular breeding - A case study with the Norway spruce defensin-like gene, Spi 1. *Silvae Genetica* 50, 75-81.
- Fossdal, C. G., Nagy, N. E., Sharma, P. & Lonneborg, A. 2003. The putative gymnosperm plant defensin polypeptide (SPI1) accumulates after seed germination, is not readily released, and the SPI1 levels are reduced in *Pythium dimorphum*-infected spruce roots. *Plant Molecular Biology* 52, 291-302.
- Fossdal, C. G., Sharma, P. & Lonneborg, A. 2003. Isolation of the first putative peroxidase cDNA from a conifer and the local and systemic accumulation of related proteins upon pathogen infection. *Plant Molecular Biology* 47, 423-435.
- Franceschi, V. R., Krokene, P., Christiansen, E. & Kreckling, T. 2005. Anatomical and chemical defences of conifer bark beetles and other pests. *New Phytologist* 167, 353-376.
- Hashimoto, J. G., Beadles-Bohling, A. S. & Wiren, K. M. 2004. Comparison of RiboGreen (R) and 18S rRNA quantitation for normalizing real-time RT-PCR expression analysis. *Biotechniques* 36, 54-60.
- Heath, M. C. 2000. Hypersensitive response-related death. *Plant Molecular Biology* 44, 321-334.
- Hietala, A. M., Kvaalen, H., Schmidt, A., Johnk, N., Solheim, H. & Fossdal, C. G. 2004. Temporal and spatial profiles of chitinase expression by Norway spruce in response to bark colonization by *Heterobasidion annosum*. *Applied and Environmental Microbiology* 70, 3948-3953.
- Hogberg, K. A., Ekberg, I., Norell, L. & von Arnold, S. 1998. Integration of somatic embryogenesis in a tree breeding programme: a case study with *Picea abies*. *Canadian Journal of Forest Research* 28, 1536-1545.
- Horton, P., Park, K.-J., Obayashi, T. & Nakai, K. 2006. In *The 4th Annual Asia Pacific Bioinformatics Conference APBC06Taipei*, Taiwan, pp. 39-48.
- Hotter, G. S. 1997. Elicitor-induced oxidative burst and phenylpropanoid metabolism in *Pinus radiata* cell suspension cultures. *Australian Journal of Plant Physiology* 24, 797-804.
- Huckelhoven, R., Dechert, C. & Kogel, K. H. 2003. Over-expression of barley BAX inhibitor 1 induces breakdown of mlo-mediated penetration resistance to *Blumeria graminis*. *Proceedings of the National Academy of Sciences of the United States Of America* 100, 5555-5560.
- Jin, W., Riley, R. M., Wolfinger, R. D., White, K. P., Passador-Gurgel, G. & Gibson, G. 2001. The contributions of sex, genotype and age to transcriptional variance in *Drosophila melanogaster*. *Nature Genetics* 29, 389-395.

- Johansson, M., Lundgren, L. & Asiegbu, F. O. 1994. In *SNS-meeting in forest pathology at Skogbrukets Kurscenter* (Ed, Aamlid, D.) Biri, Norway 9-12 August 1994, pp. 12-16.
- Johansson, S. M., Lundgren, L. N. & Asiegbu, F. O. 2004. Initial reactions in sapwood of Norway spruce and Scots pine after wounding and infection by *Heterobasidion parviporum* and *H. annosum*. *Forest Pathology* 34, 197-210.
- Johnk, N., Hietala, A. M., Fossdal, C. G., Collinge, D. B. & Newman, M. A. 2005. Defense-related genes expressed in Norway spruce roots after infection with the root rot pathogen *Ceratobasidium bicorne* (anamorph: *Rhizoctonia* sp.). *Tree Physiology* 25, 1533-1543.
- Karlsson, M., Olson, Å. & Stenlid, J. 2003. Expressed sequences from the basidiomyceteous tree pathogen *Heterobasidion annosum* during early infection of scots pine. *Fungal Genetics and Biology* 39, 31-59.
- Karonen, M., Hamalainen, M., Nieminen, R., Klika, K. D., Loponen, J., Ovcharenko, V. V., Moilanen, E. & Pihlaja, K. 2004. Phenolic extractives from the bark of *Pinus sylvestris* L. and their effects on inflammatory mediators nitric oxide and prostaglandin E-2. *Journal of Agricultural and Food Chemistry* 52, 7532-7540.
- Kirst, M., Johnson, A. F., Baucom, C., Ulrich, E., Hubbard, K., Staggs, R., Paule, C., Retzel, E., Whetten, R. & Sederoff, R. 2003. Apparent homology of expressed genes from wood-forming tissues of loblolly pine (*Pinus taeda* L.) with *Arabidopsis thaliana*. *Proceedings of the National Academy of Sciences of the United States of America* 100, 7383-7388.
- Kovalchuk, I., Titov, V., Hohn, B. & Kovalchuka, O. 2005. Transcriptome profiling reveals similarities and differences in plant responses to cadmium and lead. *Mutation Research* 570, 149-161.
- Li, G. & Asiegbu, F. O. 2004. Use of Scots pine seedling roots as an experimental model to investigate gene expression during interaction with the conifer pathogen *Heterobasidion annosum* (P-type). *Journal of Plant Research* 117, 155-162.
- Lindberg, M., Lundgren, L., Gref, R. & Johansson, M. 1992. Stilbenes and resin acids in relation to the penetration of *Heterobasidion annosum* through the bark of *Picea abies*. *European Journal of Forest Pathology* 22, 95-106.
- Manthey, K., Krajinski, F., Hohnjec, N., Firmhaber, C., Puhler, A., Perlick, A. M. & Kuster, H. 2004. Transcriptome profiling in root nodules and arbuscular mycorrhiza identifies a collection of novel genes induced during *Medicago truncatula* root endosymbioses. *Molecular Plant-Microbe Interactions* 17, 1063-1077.
- Monteiro, S., Barakat, M., Piçarra-Pereira, M. A., Teixeira, A. R. & Ferreira, R. B. 2003. Osmotin and thaumatin from grape: a putative general defense mechanism against pathogenic fungi. *Biochemistry and Cell Biology* 93, 1505-1512.
- Morel, J.-B. & Dangl, J. L. 1997. The hypersensitive response and the induction of cell death in plants. *Cell Death and Differentiation* 4, 671-683.
- Myburg, H., Morse, A. M., Amerson, H. V., Kubisiak, T. L., Huber, D., Osborne, J. A., Garcia, S. A., Nelson, C. D., Davis, J. M., Covert, S. F. & van Zyl, L. M. 2006. Differential gene expression in loblolly pine (*Pinus taeda* L.) challenged with the fusiform rust fungus, *Cronartium quercuum* f.sp. fusiforme. *Physiological and Molecular Plant Pathology* 68, 79-91.
- Nagy, N. E., Fossdal, C. G., Dalen, L. S., Lonneborg, A., Heldal, I. & Johnsen, O. 2004a. Effects of *Rhizoctonia* infection and drought on peroxidase and chitinase activity in Norway spruce (*Picea abies*). *Physiologia Plantarum* 120, 465-473.
- Nagy, N. E., Fossdal, C. G., Krokene, P., Krekling, T., Lonneborg, A. & Solheim, H. 2004b. Induced responses to pathogen infection in Norway spruce phloem: changes in polyphenolic parenchyma cells, chalcone synthase transcript levels and peroxidase activity. *Tree Physiology* 24, 505-515.
- Osborn, A. E. 1996. Preformed antimicrobial compounds and plant defense against fungal attack. *Plant Cell* 8, 1821-1831.
- Pearce, R. B. 1996. Antimicrobial defences in the wood of living trees. *New Phytologist* 132, 203-233.

- Pervieux, I., Bourassa, M., Laurans, F., Hamelin, R. & Seguin, A. 2004. A spruce defensin showing strong antifungal activity and increased transcript accumulation after wounding and jasmonate treatments. *Physiological and Molecular Plant Pathology* 64, 331-341.
- Petalidis, L., Bhattacharyya, S., Morris, G. A., Collins, V. P., Freeman, T. C. & Lyons, P. A. 2003. Global amplification of mRNA by template-switching PCR: linearity and application to microarray analysis. *Nucleic Acids Research* 31.
- Puskas, L. G., Zvara, A., Hackler, L. & Van Hummelen, P. 2002. RNA amplification results in reproducible microarray data with slight ratio bias. *Biotechniques* 32, 1330-1340.
- Ralph, S., Park, J. Y., Bohlmann, J. & Mansfield, S. D. 2006a. Dirigent proteins in conifer defense: gene discovery, phylogeny, and differential wound- and insect-induced expression of a family of DIR and DIR-like genes in spruce (*Picea* spp.). *Plant Molecular Biology* 60, 21-40.
- Ralph, S. G., Yueh, H., Friedmann, M., Aeschliman, D., Zeznik, J. A., Nelson, C. C., Butterfield, Y. S. N., Kirkpatrick, R., Liu, J., Jones, S. J. M., Marra, M. A., Douglas, C. J., Ritland, K. & Bohlmann, J. 2006b. Conifer defence against insects: microarray gene expression profiling of Sitka spruce (*Picea sitchensis*) induced by mechanical wounding or feeding by spruce budworms (*Choristoneura occidentalis*) or white pine weevils (*Pissodes strobi*) reveals large-scale changes of the host transcriptome. *Plant Cell and Environment* 29, 1545-1570.
- Reymond, P. 2001. DNA microarrays and plant defence. *Plant Physiology and Biochemistry* 39, 313-321.
- Savard, L., Li, P., Strauss, S. H., Chase, M. W., Michaud, M. & Bousquet, J. 1994. Chloroplast and nuclear gene-sequences indicate late pennsylvanian time for the last common ancestor of extant seed plants. *Proceedings of the National Academy of Sciences of the United States of America* 91, 5163-5167.
- Seth, D., Gorrell, M. D., McGuinness, P. H., Leo, M. A., Lieber, C. S., McCaughan, G. W. & Haber, P. S. 2003. SMART amplification maintains representation of relative gene expression: quantitative validation by real time PCR and application to studies of alcoholic liver disease in primates. *Journal of Biochemical and Biophysical Methods* 55, 53-66.
- Silberbach, M., Huser, A., Kalinowski, J., Puhler, A., Walter, B., Kramer, R. & Burkovski, A. 2005. DNA microarray analysis of the nitrogen starvation response of *Corynebacterium glutamicum*. *Journal of Biotechnology* 119, 357-367.
- Somssich, I. E. & Hahlbrock, K. 1998. Pathogen defence in plants - a paradigm of biological complexity. *Trends in Plant Science* 3, 86-90.
- Stasolla, C., Bozhkov, P. V., Chu, T. M., Van Zyl, L., Egertsdotter, U., Suarez, M. F., Craig, D., Wolfinger, R. D., Von Arnold, S. & Sederoff, R. R. 2004. Variation and transcript abundance during somatic embryogenesis in gymnosperms. *Tree Physiology* 24, 1073-1085.
- Stasolla, C., van Zyl, L., Egertsdotter, U., Craig, D., Liu, W. B. & Sederoff, R. R. 2003. The effects of polyethylene glycol on gene expression of developing white spruce somatic embryos. *Plant Physiology* 131, 49-60.
- Stenlid, J. 1985. Population structure of *Heterobasision annosum* as determined by somatic incompatibility, sexual incompatibility and isozyme patterns. *Canadian Journal of Botany* 63, 2268-2273.
- Stephens, C., Kazan, K., Goulter, K. C., Maclean, D. J. & Manners, J. M. 2005. The mode of action of the plant antimicrobial peptide MiAMP1 differs from that of its structural homologue, the yeast killer toxin WmKT. *FEMS Microbiology Letters* 243, 205-210.
- Takahama, U. & Oniki, T. 2000. Flavonoids and some other phenolics as substrates of peroxidase: Physiological significance of the redox reactions. *Journal of Plant Research* 113, 301-309.
- van Zyl, L., von Arnold, S., Bozhkov, P., Chen, Y. Z., Egertsdotter, U., MacKay, J., Sederoff, R. R., Shen, J., Zelena, L. & Clapham, D. H. 2002. Heterologous array analysis in Pinaceae: hybridization of *Pinus taeda* cDNA arrays with cDNA from needles and embryogenic cultures of *P. taeda*, *P. sylvestris* or *Picea abies*. *Comparative and Functional Genomics* 3, 306-318.

- Wadenback, J., Clapham, D. H., Craig, D., Sederoff, R., Peter, G. F., von Arnold, S. & Egertsdotter, U. 2005. Comparison of standard exponential and linear techniques to amplify small cDNA samples for microarrays. *BMC Genomics* 6.
- Watkinson, J. I., Sioson, A. A., Vasquez-Robinet, C., Shukla, M., Kumar, D., Ellis, M., Heath, L. S., Ramakrishnan, N., Chevone, B., Watson, L. T., van Zyl, L., Egertsdotter, U., Sederoff, R. R. & Grene, R. 2003. Photosynthetic acclimation is reflected in specific patterns of gene expression in drought-stressed loblolly pine. *Plant Physiology* 133, 1702-1716.
- Whetten, R. W., MacKay, J. J. & Sederoff, R. R. 1998. Recent advances in understanding lignin biosynthesis. *Annual Review of Plant Physiology and Plant Molecular Biology* 49, 585-609.
- Wilhelm, J., Moyal, J. P., Best, J., Kwapiszewska, G., Stein, M. M., Seeger, W., Bohle, R. M. & Fink, L. 2006. Systematic comparison of the T7-IVT and SMART-based RNA preamplification techniques for DNA microarray experiments. *Clinical Chemistry* 52, 1161-1167.
- Wolfinger, R. D., Gibson, G., Wolfinger, E. D., Bennett, L., Hamadeh, H., Bushel, P., Afshari, C. & Paules, R. S. 2001. Assessing gene significance from cDNA microarray expression data via mixed models. *Journal of Computational Biology* 8, 625-637.
- Woodward, S., Stenlid, J., Karjalainen, R. & Hüttermann, A. 1998. *Heterobasidion annosum: Biology, Ecology, Impact and Control*. CAB International, London. pp. 589.
- Yabe, T., YamadaOkabe, T., Kasahara, S., Furuichi, Y., Nakajima, T., Ichishima, E., Arisawa, M. & YamadaOkabe, H. 1996. HKR1 encodes a cell surface protein that regulates both cell wall beta-glucan synthesis and budding pattern in the yeast *Saccharomyces cerevisiae*. *Journal of Bacteriology* 178, 477-483.
- Yuen, T., Wurmbach, E., Pfeffer, R. L., Ebersole, B. J. & Sealfon, S. C. 2002. Accuracy and calibration of commercial oligonucleotide and custom cDNA microarrays. *Nucleic Acids Research* 30, e48.

Tables

Table 1. Functional classification of 179 ESTs differentially expressed by *P. sylvestris* roots infected with a pathogenic fungus *H. annosum* at 1, 5 or 15 d.p.i. as compared to un-infected control ^a

Contig number	Gene ID ^b	Putative function	Fold change			Cluster
			1 dpi	5 dpi	15 dpi	
Metabolism						
	NXCI_026_F05	glycine dehydrogenase (decarboxylating)			-1.6	1
14	NXCI_027_G06	myo-inositol 1-phosphate synthase			-1.6	1
14	NXSI_121_A05	myo-inositol 1-phosphate synthase			-1.5	1
	NXNV_162_C02	peroxidase (EC 1.11.1.7) [secretory, cationic]			-1.5	1
	NXSI_144_E08	putative lipase			-1.5	1
	NXNV_164_H08	putative xyloglucan endotransglycosylase			-1.7	1
	NXSI_031_H03	serine carboxypeptidase III precursor			-1.7	1
	NXSI_092_E10	thiazole biosynthetic enzyme precursor			-2.0	1
	NXCI_155_E06	transketolase (EC 2.2.1.1) Tkt1 precursor, chloroplast			-1.4	1
	NXSI_082_H01	endoxyloglucan transferase			1.6	2
	ST 13 H06	lucoanthocyanidin dioxygenase			1.4	2
	NXSI_025_H02	alpha-pinene synthase			-1.4	3
	NXSI_061_G02	putative peroxidase			-1.9	3
	NXNV_164_G08	3-deoxy-d-arabino-heptulosonate 7-phosphate synthase			1.6	4
	NXCI_116_D01	2-dehydro-3-deoxyphosphoheptonate aldolase			1.7	4
	ST 24 C06	5-methyltetrahydropteroyltriglutamate (methionine synthase)			1.5	4
6	NXSI_027_G10	5-methyltetrahydropteroyltriglutamate-homocysteine S-methyltransferase (methionine synthase 2)			1.7	4
6	NXSI_108_D12	5-methyltetrahydropteroyltriglutamate-homocysteine S-methyltransferase (methionine synthase 2)			1.6	4
	NXCI_066_H04	acetoacyl-CoA-thiolase		2.0	1.7	4

2	NXCI_053_F03	adenosylhomocysteinase (EC 3.3.1.1)			1.8	4
2	NXCI_122_H05	adenosylhomocysteinase (EC 3.3.1.1)			1.8	4
	NXSI_103_H03	S-adenosyl-L-homocysteine hydrolase (adenosylhomocysteinase)			1.5	4
	NXCI_149_C10	anthranilate N-benzoyltransferase			1.8	4
	NXNV_125_E12	aspartate aminotransferase, mitochondrial			1.4	4
	ST 23 F07	ATP-citrate-lyase	1.6		1.9	4
	NXCI_165_H04	cinnamoyl CoA reductase			1.7	4
4	ST 02 B03	cinnamyl-alcohol dehydrogenase	1.6		2.4	4
	NXSI_104_E01	coumarate 3-hydroxylase	1.5		1.8	4
	NXCI_122_A09	enolase (EC 4.2.1.11)			1.4	4
	NXCI_075_D09	epoxide hydrolase			1.5	4
	NXSI_127_C02	laccase			1.8	4
10	NXCI_046_E05	laccase (diphenol oxidase)			3.1	4
10	NXNV_066_B07	laccase (diphenol oxidase)			3.9	4
	NXNV_067_B05	laccase (diphenol oxidase)			2.4	4
	NXSI_008_D10	laccase (diphenol oxidase)			1.9	4
	NXNV_158_A11	methylenetetrahydrofolate reductase			1.6	4
	ST 21 G10	oxidoreductase, acting on paired donors, with incorporation or reduction of molecular oxygen (flavonone 3 hydroxylase like)			1.5	4
	NXCI_018_A08	pectate lyase 1			1.5	4
	NXSI_029_F11	pectinesterase homolog			1.5	4
8	NXSI_012_D08	peroxidase (EC 1.11.1.7)	1.4	2.8	3.4	4
8	NXSI_028_B10	peroxidase ATP 4 (EC 1.11.1.7)	1.4	2.2	4.8	4
	NXNV_031_G03	peroxidase (EC 1.11.1.7) 1 precursor			1.6	4
	NXCI_093_H05	phenylalanine ammonia-lyase (EC 4.3.1.5)		1.5	2.1	4
	NXNV_066_E09	phenylcoumaran benzylic ether reductase			1.7	4
	NXNV_158_G06	phosphoserine aminotransferase			1.5	4
	NXSI_013_B10	pinorexinol-lariciresinol reductase	1.7		1.7	4

	NXCI_064_E04	prephenate dehydratase (EC 4.2.1.51)		1.5	4
	NXSI_116_A09	putative adenosine kinase		1.8	4
	NXSI_083_G03	putative lipase (catalytic hydrolase)		1.4	4
1	NXCI_050_B07	S-adenosyl-L-methionine synthetase		1.8	4
9	NXSI_012_H05	S-adenosylmethionine synthetase	1.6	1.7	4
9	NXSI_060_E02	S-adenosylmethionine synthetase		1.8	4
	NXNV_008_F05	S-adenosylmethionine synthetase		1.7	4
	NXCI_055_D02	SRG1 protein (anthocyanidin synthase)	1.8	3.4	4
5	ST 23 G12	trans-cinnamate 4-monooxygenase	1.6	2.2	4
	NXCI_066_A11	thiamine biosynthetic enzyme 1-2 precursor		-1.7	5
	NXCI_093_B07	trans-cinnamate 4-hydroxylase (EC 1.14.13.11)		-1.8	5
	NXCI_082_E07	xyloglucan endo-transglycosylase.		-1.7	5
	NXCI_047_C05	3-deoxy-d-arabino-heptulosonate 7-phosphate synthase		1.8	6
4	NXNV_083_A10	cinnamyl alcohol dehydrogenase	1.6	1.8	6
	NXNV_164_D05	IAA-ALA hydrolase		1.6	6
	NXCI_002_E07	leucoanthocyanidin reductase		1.9	6
	NXNV_091_A04	pectin methylesterase isoform alpha		1.7	6
1	ST_21_H03	S-adenosyl-L-methionine synthetase	1.5	1.9	6
5	NXCI_087_F07	trans-cinnamate-4-hydroxylase		1.8	6
	NXSI_134_E09	pectate lyase		1.5	7
	NXCI_125_F11	pectate lyase 2		1.9	7
	NXSI_100_F02	pectin methylesterase-like		1.4	7
	ST 34 F04	putative cinnamoyl CoA reductase		1.8	7
Energy acquisition					
	NXSI_134_C01	glyceraldehyde 3-phosphate dehydrogenase		-1.5	1
	NXSI_113_B09	heme oxygenase 1 (Ho1)		-1.6	1
	NXSI_012_D03	photosystem II 10 kDa polypeptide precursor		-1.8	1
	NXNV_098_D05	NADH dehydrogenase (ubiquinone)		1.9	2

	ST 26 D05	ATP synthase C-chain	-1.5	3
15	NXCI_136_A08	basic blue protein	-1.5	3
15	NXNV_153_F09	basic blue protein - cucumber	-1.5	3
	ST 36 A10	chlorophyll a/b binding pro	-1.9	3
	ST_21_E01	FAD binding, oxidoreductase, acting on CH-OH group of donors	-1.6	3
13	NXSI_104_B11	ferredoxin precursor	-2.0	3
13	ST 39 F03	ferredoxin precursor	-1.9	3
	ST 12 D01	photosystem I reaction center subunit	-1.6	3
	NXCI_008_C01	photosystem II oxygen-evolving complex protein	-1.9	3
	NXCI_085_E04	subunit of photosystem I	-2.2	3
	NXCI_020_A08	type 2 light-harvesting chlorophyll a/b-binding protein	-1.4	3
	NXCI_084_G02	alcohol dehydrogenase (EC 1.1.1.1)	1.6	4
	NXSI_064_B03	cytochrome b5 isoform cb-5	1.4	4
	NXNV_063_A09	cytochrome c	1.6	4
	NXSI_012_H11	malate synthase-like protein	1.7	4
	NXCI_075_E11	mitochondrial nadh:ubiquinone oxidoreductase	1.9	4
	NXCI_037_F08	putative adenosine kinase	1.4	4
Cell cycle and DNA processing				
	NXSI_063_G10	CDC2PNC protein, cyclin dependent kinase	-1.4	1
Transcription				
	NXCI_012_H07	probable transcription factor Sf3	-1.4	1
	NXNV_186_D12	ring zinc finger protein	-1.5	1
Protein fate (folding, modification, destruction)				
	NXSI_061_D05	RUB1 conjugating enzyme (ubiquitin conjugating enzyme)	-1.5	1
	ST 12 G05	subtilisin serine protease	-1.5	1
	NXCI_132_B11	26s proteasome subunit	1.6	2
	ST_14_H04	cysteine proteinase	-1.5	3

	NXSI_126_A05	heat shock protein 70		-1.4	3
	ST 38 H03	peptidyl proline isomerase		1.5	4
	NXNV_117_F05	polyubiquitin	1.5	1.4	4
	NXCI_153_G06	heat shock protein 70		1.6	6
Transport					
	NXSI_112_B07	aquaporin, tonoplast intrinsic protein, delta type	-1.4	-2.1	1
11	NXSI_066_E05	tonoplast intrinsic protein BOBTIP26-1		-1.5	1
11	NXSI_055_F10	tonoplast intrinsic protein BOBTIP26-1		-1.5	1
	NXSI_089_H07	nonspecific lipid-transfer protein precursor		-1.6	3
	NXNV_098_G03	probable potassium transport protein		-1.7	3
	NXSI_089_E03	vacuolar pyrophosphatase		1.6	4
Communication and signal transduction					
	NXSI_121_B09	protein kinase/protein serine/threonine kinase		-1.4	3
	NXCI_116_H06	putative purple acid phosphatase precursor; protein serine/threonine phosphatase]		-1.5	3
	NXSI_052_E09	NBS/LRR disease resistance protein		-1.5	5
Cell rescue and defence					
	ST 04 C10	chitinase		-1.7	1
	NXNV_162_H07	thioredoxin H		-2.1	3
	ST 04 G06	antimicrobial peptide	1.6		4
	NXSI_121_H06	chitinase 1 precursor		1.7	4
	NXCI_085_H12	glutathione S-transferase	1.6		4
	ST_35_A01	metallothionein-like protein		1.8	4
	NXSI_064_A03	thaumatin	1.5	1.8	3.0
	NXCI_149_F01	thioredoxin H-type		1.5	6
7	ST 31 D06	glutathione transferase		1.5	8
7	NXSI_142_E03	glutathione transferase (EC 2.5.1.18)		1.5	8
Cell fate					

	NXNV_083_H11	BAX inhibitor-1 like	-1.6	1	
		System regulation of interaction with environment			
	NXCI_093_F03	abscisic acid water deficit stress and ripening inducible	-1.7	1	
	NXSI_134_D02	aluminum-induced protein	-1.5	1	
	ST 07 A03	aquaporin	-1.5	-2.1	1
	ST 37 E10	gibberellin regulated protein	-1.6		1
	NXSI_076_G02	multiple stress-responsive zinc-finger protein	-1.8		1
	NXSI_131_C03	putative aba induced plasma membrane protein	-1.5		1
12	NXCI_135_H12	water deficit inducible Lp3-like	-2.3		1
	NXCI_132_H04	water-stress-inducible protein Lp3-like	-2.4		1
	NXSI_107_G10	temperature induced lipocalin	-1.5		3
12	ST 23 A08	water deficit inducible protein Lp3	-1.8		3
	NXNV_133_D04	early response to drought 3	1.7		4
	NXNV_158_D06	luminal binding protein 3 (glucose-regulated protein)	1.5		4
	NXSI_055_F08	putative auxin-induced protein	1.4		4
	NXSI_065_F06	auxin-induced Atb2	1.5		6
	ST 23 G07	putative auxin-induced protein	1.4		6
	NXSI_055_B06	GASA5-like protein.	1.5		7
		Development			
	NXSI_102_E12	similarity to nodulin	-1.5		1
	ST 40 D05	dormancy associated protein	-1.7		3
	NXCI_021_G04	putative late embryogenesis abundant	-2.0		3
	NXCI_067_A10	highly similar to developmental protein DG1118	-1.5		8
		Cell, tissue and organ differentiation			
	NXCI_029_H07	kinesin light chain	1.5		6
	NXNV_151_A07	expansin like	-1.7		1
	NXSI_098_C01	annexin	-1.5		8
		Unclassified proteins and unknown function			

	ST 27 G01	no hit		-1.5	1
	ST 28 F04	no hit		-1.4	1
	ST 34 H09	no hit		-1.5	1
	NXCI_027_E04	no hit		-1.6	1
	NXCI_083_F01	no hit		-1.7	1
	NXNV_066_D07	no hit	-1.5	-2.0	1
	NXNV_129_E04	no hit		-2.0	1
	NXNV_130_C10	no hit	-1.5	-1.9	1
	NXNV_134_H10	no hit		-1.5	1
	NXSI_087_D08	no hit		-1.6	1
	NXCI_055_D01	putative surface protein, endosperm specific	-1.4	-1.9	1
	NXSI_005_F10	no hit		1.5	2
	NXSI_077_E09	putative arabinogalactan/proline-rich protein		1.5	2
	ST 07 A05	no hit		-1.4	3
	ST 19 A12	no hit		-1.7	3
	NXCI_009_A10	no hit		-1.4	3
	NXCI_155_G05	no hit		-2.1	3
	NXSI_055_H08	no hit		-1.6	3
	ST 27 A08	no hits		-1.4	3
	NXNV_046_H05	arabinogalactan protein	1.4	3.7	4
3	NXNV_081_D10	no hit		1.4	4
	ST 25 C07	no hit	1.5	1.5	4
	NXCI_117_C07	no hit		1.5	4
	NXNV_044_F10	no hit		2.1	4
	NXSI_114_A04	no hit		1.7	4
	ST 11 D05	unknown		1.4	4
	NXCI_029_F09	unknown	1.7	2.6	4
3	NXSI_051_B09	no hit		1.8	6

NXCI_069_A02	no hit		2.3	6
ST 32 G03	no hits		1.6	6
NXNV_125_G04	no hit		1.7	7
ST_08_A10	no hit		1.5	7
ST 07 E10	unknown	1.4		7
ST 07 F11	hypothetical protein		-1.5	8
NXSI_021_D01	no hit		-1.5	8

^a The ESTs were determined by the mixed model analysis to be differentially expressed if the fold change was ≥ 1.4 or ≤ -1.4 . All the differentially expressed ESTs were divided into 8 regulatory patterns, indicated by the numbers 1-8. The ESTs forming contigs were marked with numbers 1-15. Some of the ESTs could have been prescribed to more than one functional group.

^b The gene ID can be used to retrieve ESTs sequences from the GeneBank or the database at <http://biodata.ccgb.umn.edu/>

Table 2. Fold changes of selected genes transcripts determined by real-time RT-PCR in *P. sylvestris* root tissues infected with *H. annosum* at 1, 5 or 15 d.p.i. as compared to uninfected control^a.

Gene ID	Putative function	Array	Real-time RT-PCR ^b		
1 d.p.i.					
ST 04 G06	antimicrobial peptide	1.6	4.6	±	3.5
NXSI_012_D08	peroxidase	1.4	2.0	±	0.3
NXSI_012_H05	S-adenosylmethionine synthase	1.0	1.1	±	0.1
NXSI_064_A03	thaumatin	1.5	20.9	±	6.3
ST_07_E10	unknown	1.4	2.6	±	0.6
NXCI_082_D08	unknown	-1.3 ^c	-4.1	±	0.3
NXSI_001_G04	no hit	-1.5 ^c	-5.6	±	2.6
NXSI_054_F05	glycine-rich protein	1.6 ^c	2.6	±	0.7
ST_03_F07	hypothetical protein	1.3 ^c	3.4	±	1.9
5 d.p.i.					
ST 04 G06	antimicrobial peptide	1.3 ^c	3.0	±	1.9
NXSI_012_D08	peroxidase	3.0	17.1	±	7.8
NXSI_012_H05	S-adenosylmethionine synthase	1.7	7.6	±	3.6
NXSI_064_A03	thaumatin	1.9	24.3	±	18.3
NXCI_066_H04	acetoacetyl CoA thiolase	2.1	4.3	±	1.2
ST_02_B03	cinnamoyl alcohol dehydrogenase	1.6	7.5	±	6.4
15 d.p.i.					
ST 04 G06	antimicrobial peptide ^d		4.8	±	4.8
NXSI_012_D08	peroxidase	3.4	24.8	±	20.7
NXSI_012_H05	S-adenosylmethionine synthase	1.7	14.7	±	3.7
NXSI_064_A03	thaumatin	3.0	22.5	±	10.7
NXCI_066_H04	acetoacetyl CoA thiolase	1.7	2.0	±	1.0
ST_02_B03	cinnamoyl alcohol dehydrogenase	2.4	4.5	±	2.9
NXCI_018_G04	aldehyde dehydrogenase	-1.4	-5.2	±	4.1
NXNV_162_H07	thioredoxin	-2.1	-2.0	±	0.6
NXSI_082_H01	xyloglucan endotransglycosylase	-1.7	-15.4	±	12.9

^a Distribution of number of copies of biological replicates is presented in Supplementary materials Figure S1.

^b Fold changes determined by real-time RT-PCR ± standard deviation.

^c Fold changes determined by the array for antimicrobial peptide 15 d.p.i. were not significant.

^d Fold changes were calculated as average of two biological replicates (see Supplementary Table S1).

Supplementary materials

The data discussed in this publication have also been deposited at NCBI Gene Expression Omnibus (GEO, <http://www.ncbi.nlm.nih.gov/geo/>) and are accessible through GEO platform GPL4039, series accession numbers: GSE5407, GSE5408 and GSE5410. The following supplementary material accompanies the manuscript and is available in electronic form on the journal website:

Table S1. Genes differentially expressed selected with lower stringency.

Table S2. Primers used for the real-time RT-PCR experiment.

Figure S1. Distribution of number of transcripts determined by real-time RT-PCR in control pine roots and infected with *H. annosum* at 1, 5 or 15 d.p.i. Each dot represents a biological replicate consisting of three technical replicates. Bar represents mean copy number. Abbreviations: AMP-antimicrobial peptide ST_04_G06, AACT-acetoacetyl CoA thiolase NXCI_066_H04, CAD-cinnamoyl alcohol dehydrogenase ST_02_B03, ALD – aldehyde dehydrogenase NXCI_018_G04, GLYRICH-glycine rich protein NXSI_054_F05, POX-peroxidase NXSI_012_D08, SAM-S-adenosylmethionine synthase NXSI_012_H05, THAU-thaumatococin NXSI_064_A03, THIO-thioredoxin NXNV_162_H07, UNK3-no hit NXSI_001_G04, UNK4-hypothetical protein ST_03_F07, UNK5-unknown ST_07_E10, UNK6-unknown NXCI_082_D08, XGE-xyloglucan endotransglycosylase NXSI_082_H01.